International Journal of Innovative Solutions in Engineering
2026, Vol. 2 No. 2 (pages 73–81)
DOI: 10.47960/3029-3200.2026.2.2.73

Research Article

OPEN ACCESS

# Mechanical Properties and Microstructural Characterization of WAAM-Deposited Duplex 2205 Stainless Steel

Nikola Knezović[1], Angela Topić[1], Ivica Garašić[2]

[1]Faculty of Mechanical Engineering, Computing and Electrical Engineering University of Mostar, Bosnia and Herzegovina
[2]Faculty of Mechanical Engineering and Naval Architecture University of Zagreb, Croatia

**Abstract**

This study investigates the mechanical properties and microstructural characteristics of Duplex 2205 stainless steel deposited via Wire-and-Arc Additive Manufacturing (WAAM), a material widely used in demanding applications for its superior mechanical properties and corrosion resistance. A single-bead wall was produced using selected process parameters based on process stability and arc energy requirements, and subsequently evaluated for surface quality, bead appearance, and overall morphology. Microstructural analysis was conducted to assess the austenite/ferrite phase ratio, while mechanical performance was evaluated using microhardness, tensile strength, and impact toughness tests. The results provide a comprehensive insight into the structural integrity and performance of WAAM-deposited Duplex 2205 stainless steel.

**Article history**

Received: 27.5.2026.
Revised: 8.6.2026.
Accepted: 19.6.2026.

**Keywords**

Wire-Arc Additive Manufacturing,
Welding,
2205 Duplex Stainless Steel,
Microstructure,
Mechanical Properties.

## 1 Introduction

Modern industrial demands have driven continuous research into innovative manufacturing technologies. One such development is additive manufacturing, which has gained considerable momentum due to its capacity to produce complex components with enhanced efficiency. Before the emergence of Wire and Arc Additive Manufacturing (WAAM), however, most additive manufacturing techniques were not well-suited for the production of metal parts. WAAM combines welding principles with additive manufacturing concepts, using an electric arc as the heat source and welding wire as feedstock, with the process guided by robotic systems or CNC machines [1, 2]. Although the first WAAM patent was filed as early as 1925 [3], broader research interest in the technology emerged only after its potential to reduce material waste in the aerospace industry was recognized [4]. Consequently, a significant portion of research has focused on the production of aerospace components, which has largely determined material selection, with titanium, aluminum, and nickel-based alloys being the most prevalent [5]‑[9]. As interest in WAAM expands globally, an increasingly diverse range of metals and alloys is being processed using this technology. A notable advantage over conventional manufacturing methods is its capacity to produce functionally graded materials (FGM) – composites characterized by a gradual variation in composition, microstructure, or properties across their volume [9, 10].

Despite the expanding material scope of WAAM, duplex stainless steels remain relatively underrepresented in the literature compared to more commonly studied alloys such as titanium and aluminum [12]‑[15]. This is largely attributable to the inherent challenges of welding these steels, as duplex stainless steels require precise control of heat input and interpass temperature to maintain the desired austenite/ferrite phase balance. The welding thermal cycle must be carefully managed, as both excessive and insufficient heat input can disrupt microstructural equilibrium. Overheating may promote the formation of detrimental intermetallic phases such as sigma phase [16], while insufficient

**Contact** Nikola Knezović, nikola.knezovic@fsre.sum.ba, Faculty of Mechanical Engineering, Computing and Electrical Engineering University of Mostar, Bosnia and Herzegovina

heat input can result in an undesirable ferrite-dominated microstructure [15, 16]. Both scenarios lead to degradation of the mechanical properties and corrosion resistance that make duplex stainless steels particularly attractive. The complexity of processing these steels has therefore significantly limited WAAM-related research, leaving considerable scope for further investigation.

This study investigates the mechanical properties and microstructural characterization of WAAM-deposited Duplex 2205 stainless steel. The key novelty of this work lies in the systematic comparison of the mechanical properties obtained with relevant material standards, assessing whether WAAM-deposited Duplex 2205 meets the requirements prescribed for conventionally produced counterparts. To the best of the authors' knowledge, such a direct and systematic comparison against applicable material standards has not been previously reported in the literature for this material‐process combination.

## 2 Methodology

The WAAM wall was produced using a robotic welding station manufactured by Daihen Varstroj (Lendava, Slovenia), consisting of an OTC Almega AX-V6 six-axis robotic arm with a maximum working range of 3.14 $m^2$, an AX-C motion controller, and a CM-7401 wire feeder. The MIG welding power source used was the DP-400 unit, suitable for welding stainless steels, with a current range of 30–400 A and a voltage range of 12–38 V.

A grade 1.4301 (AISI 304 or X5CrNi18-10), austenitic stainless steel plate, 8 mm thick, was used as the base material. To minimize distortion, the base plate was welded to a 15 mm-thick mild-steel backing plate before deposition. The filler material was Avesta 2205 welding wire (EN ISO 14343-A: G 22 9 3 NL), with a diameter of 1.2 mm, primarily intended for welding Duplex 2205 (1.4462) stainless steel. The wire was manufactured by MIG WELD GmbH International (Landau/Isar, Germany).

A shielding gas mixture of 98% argon and 2% nitrogen was used throughout the deposition process. Nitrogen acts as a strong austenite stabilizer, promoting the desired austenite/ferrite phase balance during solidification while suppressing unwanted phase transformations and preserving the corrosion resistance characteristic of duplex stainless steels.

Interpass temperature was monitored using the Fluke 568 infrared and contact thermometer. An interpass temperature of 50 °C was maintained between successive layers to prevent excessive heat accumulation and the associated risk of microstructural changes and distortion. Lower interpass temperatures were not considered because they would significantly increase the overall deposition time.

## 3 Process Parameter Optimization and Wall Deposition Procedure

The deposition process required a stable arc and a minimum bead width of 7 mm, the latter of which was defined by dimensional requirements for subsequent material characterization and testing. A minimum wall height of 60 mm and length of 300 mm were also specified on the same basis. Unlike bead width, these two dimensions are not directly governed by the selected process parameters, as the desired height and length can be achieved by adjusting the number of deposited layers and the programmed path length, respectively.

According to the literature [15, 17], the minimum recommended arc energy for this duplex stainless steel grade is 0.4 kJ/mm, calculated according to Equation 1, where I is the welding current (A), U is the voltage (V), and v is the travel speed (mm/min).

$$AE = \frac{I \cdot U \cdot 60}{v \cdot 1000}\ [kJ/mm] \qquad \text{Eq 1}$$

Preliminary trials were conducted with varying combinations of welding current, voltage, and travel speed. Of all parameter sets tested, four satisfied the minimum bead width requirement of 7 mm. Based on the trial results, a parameter set of 130 A, 16–18 V, and 250 mm/min travel speed was selected for wall deposition. The remaining three parameter sets were rejected due to process instability, uneven bead geometry, and surface irregularities.

It should be noted that the current and voltage values are nominal, as the power source continuously adjusted these parameters during deposition; however, such variations were negligible and did not compromise the minimum arc energy requirement. During the deposition of the second layer, process instabilities and surface irregularities reappeared, likely due to reduced heat dissipation in subsequent layers – whereas heat is rapidly conducted through the base plate during the first layer, later layers rely on the previously deposited material as the primary heat sink. This was addressed by incrementally increasing the travel speed to 260 mm/min in the second layer and 270 mm/min in the third layer, restoring process stability and eliminating surface irregularities. The minimum arc energy requirement remained satisfied throughout, with a calculated value of 0.49 kJ/mm at 270 mm/min. Following this correction, all parameters were finalized and entered into the robot control program. Before deposition, the austenitic stainless steel base plate was wire-brushed and cleaned with a 96% ethanol solution. Layers were deposited sequentially, with each successive layer initiated from the side where the previous one ended, ensuring uniform material distribution and avoiding localized build-up. As the average layer height ranged from 2 to 2.5 mm, the robotic arm was raised by approximately that amount after each layer. A total of 30 layers were deposited, yielding a wall height of 64 mm. The completed wall, shown in Figure 1, was produced in 132 minutes.

Figure 1 Final appearance of the deposited WAAM wall

## 4 Results and discussion

The deposited wall maintained a perpendicular orientation relative to the substrate throughout the entire build, with no lateral deviation observed, confirming the suitability of the robotic system for this type of application. Minor distortion was noted, as the progressive accumulation of layers caused upward bending of the substrate ends despite rigid clamping, resulting in a wall approximately 1–2 mm taller at the ends than at the center. Since the outermost layers were excluded from further analysis, this effect was not considered critical. Residual stresses were beyond the scope of this study and are identified as an important subject for future investigation.

The most prominent defect identified through visual inspection was porosity. Pore clusters were predominantly found on the outer wall surfaces, with a higher concentration in the upper regions. This distribution suggests a progressive reduction in shielding gas effectiveness at greater build heights, as the gas tends to disperse into the surrounding atmosphere. In the lower layers, the substrate acts as a physical barrier that deflects the shielding gas, providing more effective protection. Additional contributing factors may include buoyancy-driven air currents rising along the heated wall surface and disrupting the gas envelope, as well as increased travel speed, which may reduce shielding gas coverage [19].

These remain hypotheses, but each represents a worthwhile direction for future study. Porosity reduction is among the most important targets for process improvement, and relevant strategies can be found in [19, 20], where purpose-built shielding gas enclosures were employed to improve protection during deposition.

Following the initial visual inspection, the wall was machined to remove the outer surface layer and expose the internal material.

Microstructural analysis was performed at 15 points along the height of the deposited wall's cross-section, with the two lowermost points excluded from averaging – one corresponding to the base material and the other to the fusion zone. The phase balance was assessed using two complementary methods: a ferrite meter and image analysis software applied to optical microscopy images. When averaged across all measurement points, the ferrite meter yielded a mean value of approximately 38 FN, corresponding to a ferrite content of roughly 35–36% [22]. Image analysis software returned a slightly higher value of approximately 38.5%. The discrepancy between the two methods is likely attributable to the limitations of optical microscopy, as the image quality achievable with this technique may not be sufficient for precise phase boundary discrimination, potentially introducing error in the software-based analysis. Although the two methods yielded slightly different values, both indicate a ferrite content somewhat lower than the nominal value declared for the filler wire (approximately 50%). This reduction is likely attributable to the elevated nitrogen content in the shielding gas, as nitrogen is a strong austenite stabilizer. However, given that the nitrogen proportion was relatively modest, the resulting decrease in ferrite content was not substantial. Figure 2 shows the microstructure of a representative section of the deposited wall. The microstructure is predominantly characterized by a dendritic morphology with ferritic laths, typical of arc-based additive manufacturing processes. Grains are elongated in the build direction, having coalesced during repeated thermal cycles inherent to the layer-by-layer deposition process, and are predominantly austenitic. Certain grains exhibit refinement resulting from reheating upon deposition of subsequent layers, with preferential lateral growth observed rather than growth in the build direction. The described anisotropic microstructure suggests that the mechanical properties in the vertical and horizontal directions are likely to differ, which is an important consideration when evaluating the performance of WAAM-deposited components.

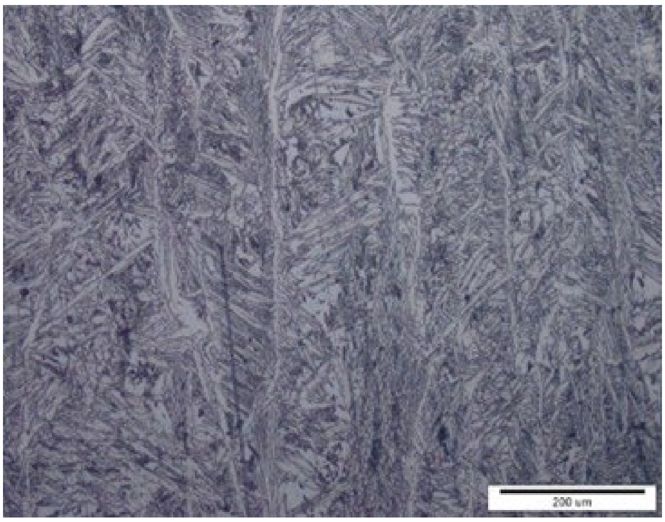


Figure 2 Microstructure of the deposited WAAM wall

Although sigma phase was identified in the Introduction as a potential concern in WAAM processing of duplex stainless steels, its presence could not be conclusively confirmed or excluded using optical microscopy alone. Given the localized nature of sigma phase precipitation, it is possible that microhardness indentations did not capture affected regions; however, the uniform hardness distribution recorded across the build height indicates that any such phase, if present, did not significantly compromise the mechanical integrity of the deposited material.

Microhardness testing was carried out using the Vickers method, following the same measurement grid as the microstructural analysis, with measurements taken at identical positions across the cross-section of the deposited wall. The microhardness profile across the deposited wall is presented in Figure 3, illustrating the distribution of hardness values along the build height.

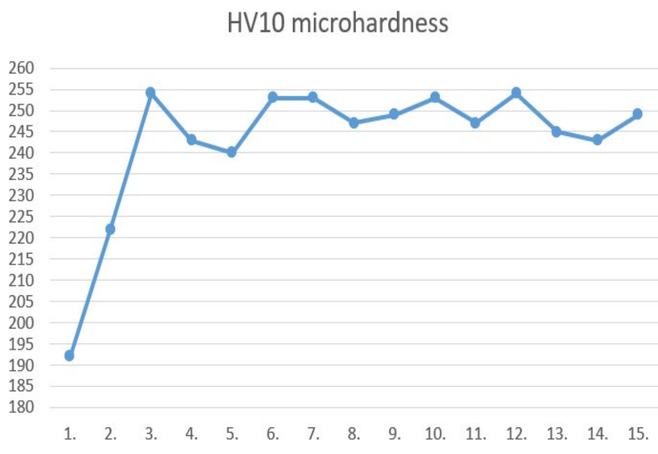


Figure 3 Microhardness profile of the deposited WAAM wall

The lower hardness values recorded at the first two measurement points are consistent with their respective positions within the base material and the fusion zone. Standards EN 10088-2 and EN 10088-4 do not specify maximum hardness requirements for this steel grade. However, EN 10088-3 and EN 10088-5 prescribe a maximum hardness of 270 HB, equivalent to approximately 277 HV, for products with a thickness below 160 mm. The measured microhardness values comply with this requirement, neither the mean value of 248 HV nor the maximum recorded value of 254 HV exceeds the prescribed limit. These results indicate that, with respect to hardness, the WAAM-deposited material meets the criteria set for conventionally produced Duplex 2205 stainless steel products.

Tensile specimens were extracted in the horizontal direction, parallel to the deposition direction, as the wall height was insufficient to accommodate specimens oriented in the build direction. Tensile testing was performed in accordance with ISO 6892-1. Figure 4 presents the stress-strain diagram obtained from tensile testing of the WAAM-deposited material. The results indicate a yield strength $R_{p0.2}$ of 540 MPa, an ultimate tensile strength $R_m$ of 749 MPa, and an elongation $A_{5.65}$ of 17%. As with hardness, the tensile properties were compared against the requirements of the relevant standards. EN 10088-2 and EN 10088-4 specify a minimum yield strength of 500 MPa and an ultimate tensile strength in the range of 700–950 MPa for cold-rolled strip, a minimum yield strength of 460 MPa and an ultimate tensile strength of 700–950 MPa for hot-rolled strip, and a minimum yield strength of 460 MPa and an ultimate tensile strength of 640–840 MPa for cold-rolled plate. The measured yield strength of 540 MPa and ultimate tensile strength of 749 MPa satisfy the requirements across all three product categories. However, the measured elongation of 17% falls short of the minimum requirements specified in the same standards. EN 10088-2 and EN 10088-4 prescribe a minimum elongation A5.65 of 20% for cold-rolled strip, and 25% for both hot-rolled strip and cold-rolled plate. The obtained value does not meet the requirements of any of the three product categories, which represents a notable limitation of the WAAM-deposited material in its current form. Such results are partially expected and are consistent with findings reported in the literature [5], [6], [23].

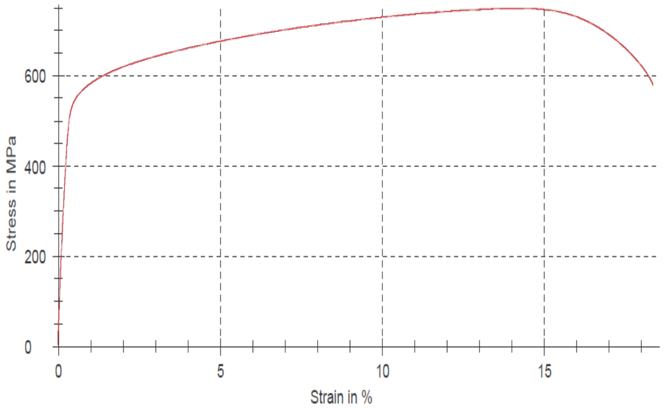


Figure 4 Stress-strain diagram of the deposited WAAM wall

Impact toughness is among the most critical mechanical properties of duplex stainless steels. As anisotropic behavior has been frequently reported in the literature, and given that the deposited wall geometry readily permitted the extraction of specimens in both orientations, impact toughness was assessed in the horizontal (L, longitudinal) and vertical (T, transverse) directions. Three specimens were extracted in each orientation, and the resulting values were compared against the relevant standards, as previously referenced in the context of microhardness and tensile testing. Charpy impact toughness testing was conducted in accordance with ISO 148-1. Table 1 shows the results of impact toughness testing. Across all four applicable standards (EN 10088-2, EN 10088-3, EN 10088-4, and EN 10088-5), the requirement for impact toughness of this duplex stainless steel grade is consistent: a minimum absorbed energy of 100 J at room temperature.

Table 1 Results of impact toughness testing

| Dir. | Spec. Nr. | $KV_{10}$ (J) | Average $KV_{10}$ (J) |
|---|---|---|---|
| L | 1 | 270.45 | 262.06 |
| | 2 | 258.56 | |
| | 3 | 257.17 | |
| T | 1 | 308.03 | 287.33 |
| | 2 | 265.84 | |
| | 3 | 288.11 | |

It is worth noting that considerably higher values have been reported in the literature for duplex stainless steels, ranging from 150 J to nearly 300 J [24, 25]. In light of these values, it is unsurprising that all specimens exhibited absorbed energy well above the minimum prescribed by the standards. Nevertheless, a notable difference in impact toughness was observed between the two orientations, which is consistent with the tensile testing results – the insufficient elongation recorded in the longitudinal direction suggests reduced ductility, which is likely reflected in the lower toughness values measured in that orientation, further confirming the anisotropic nature of the WAAM-deposited material.

## 5 Conclusion and suggestions for future research

This study examined the microstructural characteristics and mechanical properties of Duplex 2205 stainless steel deposited by Wire and Arc Additive Manufacturing (WAAM), with the principal aim of assessing whether the deposited material meets the requirements set by the relevant standards for conventionally produced Duplex 2205 products.

The deposited wall exhibited satisfactory dimensional stability throughout the build. Minor substrate distortion was observed due to progressive thermal accumulation during layer-by-layer deposition, but was considered non-critical as the outermost layers were excluded from further analysis. Porosity was identified as the most prominent defect, with pore clusters concentrated at the outer wall surfaces and in the upper regions of the deposit. This distribution is attributed to the progressive reduction in shielding gas effectiveness with increasing build height, with buoyancy-driven air currents and increased travel speed identified as potential contributing factors.

Microstructural analysis revealed a ferrite content of approximately 35-38%, notably lower than the nominal value declared for the filler wire (~50%). This reduction is attributed to the nitrogen content in the shielding gas, which acts as a strong austenite stabilizer. The microstructure exhibited a dendritic morphology with ferritic laths and grains elongated in the build direction, consistent with the repeated thermal cycling inherent to the WAAM process. Grain refinement was observed in regions subjected to reheating by subsequent layers, with preferential lateral rather than vertical growth. The resulting anisotropic microstructure was reflected in the mechanical testing results.

Microhardness measurements yielded a mean value of 248 HV and a maximum of 254 HV, both within the limit of 277 HV prescribed by EN 10088-3 and EN 10088-5. The hardness values were relatively uniform along the build height, with no pronounced gradient observed across the deposited wall, indicating consistent thermal conditions during deposition. Both the mean and maximum recorded values comply with the prescribed limit, confirming that the WAAM-deposited material meets the hardness requirements set for conventionally produced Duplex 2205 stainless steel products.

Tensile testing in the horizontal direction produced a yield strength of 540 MPa and an ultimate tensile strength of 749 MPa, satisfying the minimum requirements across all relevant product categories defined in EN 10088-2 and EN 10088-4. However, the measured elongation of 17% fell below the minimum requirements of 20-25% specified in the same standards, indicating the material's primary limitation in its as-deposited condition. This shortfall in ductility suggests that further process optimization or post-weld heat treatment may be necessary before WAAM-deposited Duplex 2205 can be considered a direct substitute for conventionally produced counterparts in applications requiring sufficient ductility.

Impact toughness was evaluated in both the horizontal (longitudinal) and vertical (transverse) orientations. All specimens substantially exceeded the minimum absorbed energy of 100 J at room temperature prescribed uniformly across EN 10088-2, EN 10088-3, EN 10088-4, and EN 10088-5. A pronounced difference in absorbed energy between the two orientations was observed, suggesting anisotropic impact-toughness behavior in the WAAM-deposited material. Since tensile testing was conducted exclusively in the horizontal direction, a definitive conclusion regarding tensile anisotropy cannot be drawn; nevertheless, the observed toughness difference between orientations indicates directional dependency in the mechanical response of the deposited material.

Overall, WAAM-deposited Duplex 2205 stainless steel demonstrated compliance with the relevant standards for hardness, yield strength, ultimate tensile strength, and impact toughness. The major contribution of this study is establishing that WAAM technology can produce Duplex 2205 components whose mechanical properties largely meet the requirements of conventionally manufactured counterparts. Elongation remains the only property that does not meet the standard requirements in the as-deposited condition, highlighting the need for further process optimization before WAAM-deposited Duplex 2205 can be considered a direct substitute in applications where ductility is a governing criterion. Based on the findings of this study, the following topics are identified as priorities for future investigation:

- Shielding gas protection strategies, including the use of purpose-built enclosures, are employed to reduce porosity, particularly in the upper regions of the wall where gas coverage was found to be least effective.
- Use of different interpass temperatures on the microstructural and mechanical properties of the deposited material, with particular focus on higher temperatures that would reduce idle time between layers and thereby increase overall deposition efficiency; such an investigation would provide practically relevant insight into the process window within which acceptable microstructural and mechanical performance can be maintained.
- Post-weld heat treatment as a potential means of improving ductility and elongation to meet standard requirements.
- Mechanical testing in the vertical (build) direction, including tensile testing, to fully characterize the anisotropic behavior of the deposited material; this direction of investigation is closely linked to the recommendation regarding interpass temperature, as producing walls of sufficient height for vertical specimen extraction would inevitably increase deposition time, which could be mitigated by adopting higher interpass temperatures.

**Conflicts of Interest**: The author(s) report there are no competing interests to declare;

**Data availability statements**: The data presented in this study are available on request from the corresponding author;

## References


[1] A. Busachi, J. Erkoyuncu, P. Colegrove, F. Martina, and J. Ding, “Designing a WAAM Based Manufacturing System for Defence Applications,” *Procedia CIRP*, vol. 37, pp. 48–53, 2015, doi: 10.1016/j.procir.2015.08.085.

[2] T. DebRoy *et al.*, “Additive manufacturing of metallic components – Process, structure and properties,” *Progress in Materials Science*, vol. 92, pp. 112–224, Mar. 2018, doi: 10.1016/j.pmatsci.2017.10.001.

[3] S. W. Williams, F. Martina, A. C. Addison, J. Ding, G. Pardal, and P. Colegrove, “Wire + Arc Additive Manufacturing,” *Materials Science and Technology*, vol. 32, no. 7, pp. 641–647, May 2016, doi: 10.1179/1743284715Y.0000000073.

[4] J. Mehnen, J. Ding, H. Lockett, and P. Kazanas, “Design study for wire and arc additive manufacture,” *IJPD*, vol. 19, no. 1/2/3, p. 2, 2014, doi: 10.1504/IJPD.2014.060028.

[5] F. Wang, S. Williams, P. Colegrove, and A. A. Antonysamy, “Microstructure and Mechanical Properties of Wire and Arc Additive Manufactured Ti-6Al-4V,” *Metall Mater Trans A*, vol. 44, no. 2, pp. 968–977, Feb. 2013, doi: 10.1007/s11661-012-1444-6.

[6] E. Brandl, B. Baufeld, C. Leyens, and R. Gault, “Additive manufactured Ti-6Al-4V using welding wire: comparison of laser and arc beam deposition and evaluation with respect to aerospace material specifications,” *Physics Procedia*, vol. 5, pp. 595–606, 2010, doi: 10.1016/j.phpro.2010.08.087.

[7] D. Ding, Z. Pan, S. Van Duin, H. Li, and C. Shen, “Fabricating Superior NiAl Bronze Components through Wire Arc Additive Manufacturing,” *Materials*, vol. 9, no. 8, p. 652, Aug. 2016, doi: 10.3390/ma9080652.

[8] C. Zhang, Y. Li, M. Gao, and X. Zeng, “Wire arc additive manufacturing of Al-6Mg alloy using variable polarity cold metal transfer arc as power source,” *Materials Science and Engineering: A*, vol. 711, pp. 415–423, Jan. 2018, doi: 10.1016/j.msea.2017.11.084.

[9] N. Knezović and A. Topić, “Innovations, Prospects, and Future Directions in Wire and Arc Additive Manufacturing,” *International Journal of Innovative Solutions in Engineering*, vol. 1, no. 1, pp. 33–39, Jan. 2025, doi: 10.47960/3029-3200.2025.1.1.33.

[10] C. Shen, Z. Pan, D. Cuiuri, J. Roberts, and H. Li, “Fabrication of Fe-FeAl Functionally Graded Material Using the Wire-Arc Additive Manufacturing Process,” *Metall Mater Trans B*, vol. 47, no. 1, pp. 763–772, Feb. 2016, doi: 10.1007/s11663-015-0509-5.

[11] O. Mehrabi, S. M. H. Seyedkashi, and M. Moradi, “Functionally Graded Additive Manufacturing of Thin-Walled 316L Stainless Steel-Inconel 625 by Direct Laser Metal Deposition Process: Characterization and Evaluation,” *Metals*, vol. 13, no. 6, p. 1108, Jun. 2023, doi: 10.3390/met13061108.

[12] W. Jin, C. Zhang, S. Jin, Y. Tian, D. Wellmann, and W. Liu, “Wire Arc Additive Manufacturing of Stainless Steels: A Review,” *Applied Sciences*, vol. 10, no. 5, p. 1563, Feb. 2020, doi: 10.3390/app10051563.

[13] N. Knezovic, A. Topic, I. Garasic, and I. Juric, “Application of Wire and Arc Additive Manufacturing for Fabrication of Duplex Stainless Steel Product,” in *DAAAM Proceedings*, 1st ed., vol. 1, B. Katalinic, Ed., DAAAM International Vienna, 2019, pp. 0599–0604. doi: 10.2507/30th.daaam.proceedings.081.

[14] N. Knezović, I. Garašić, and I. Jurić, “Influence of the Interlayer Temperature on Structure and Properties of Wire and Arc Additive Manufactured Duplex Stainless Steel Product,” *Materials*, vol. 13, no. 24, p. 5795, Dec. 2020, doi: 10.3390/ma13245795.

[15] A. Rahimi, M. Yazdizadeh, M. V. Ara, and M. Pouranvari, “CMT wire-arc additive manufacturing of 310 austenitic stainless steel: Microstructure-properties relationships,” *Journal of Materials Research and Technology*, vol. 35, pp. 881–891, Mar. 2025, doi: 10.1016/j.jmrt.2025.01.065.

[16] K. T. Nirosta, Practical Guidelines for the Fabrication of Duplex Stainless Steels. 2014.

[17] Y. Hu, Y. Shi, K. Wang, and J. Huang, “Effect of Heat Input on the Microstructure and Mechanical Properties of Local Dry Underwater Welded Duplex Stainless Steel,” *Materials*, vol. 16, no. 6, p. 2289, Mar. 2023, doi: 10.3390/ma16062289.

[18] Leif, “Welding Duplex Stainless Steels — A Review Of Current Recommendations,” *Weld World*, vol. 56, no. 5–6, pp. 65–76, May 2012, doi: 10.1007/BF03321351.

[19] K. S. Derekar, “A review of wire arc additive manufacturing and advances in wire arc additive manufacturing of aluminium,” *Materials Science and Technology*, vol. 34, no. 8, pp. 895–916, May 2018, doi: 10.1080/02670836.2018.1455012.

[20] J. Ding, P. Colegrove, F. Martina, S. Williams, R. Wiktorowicz, and M. R. Palt, “Development of a laminar flow local shielding device for wire + arc additive manufacture,” *Journal of Materials Processing Technology*, vol. 226, pp. 99–105, Dec. 2015, doi: 10.1016/j.jmatprotec.2015.07.005.

[21] Y. Ma, D. Cuiuri, H. Li, Z. Pan, and C. Shen, “The effect of postproduction heat treatment on γ-TiAl alloys produced by the GTAW-based additive manufacturing process,” *Materials Science and Engineering: A*, vol. 657, pp. 86–95, Mar. 2016, doi: 10.1016/j.msea.2016.01.060.

[22] Helmut Fischer GmbH, *FERITSCOPE® FMP30: Measurement of the Ferrite Content in Austenitic and Duplex Steel*, Tech. Brochure no. 902-039, n.d. [Online]. Available: https://helmut-fischer.gr/files/items/4/BROC_FMP30_FERITSCOPE_902-039_en.pdf

[23] E. Brandl, F. Palm, V. Michailov, B. Viehweger, and C. Leyens, “Mechanical properties of additive manufactured titanium (Ti–6Al–4V) blocks deposited by a solid-state laser and wire,” *Materials & Design*, vol. 32, no. 10, pp. 4665–4675, Dec. 2011, doi: 10.1016/j.matdes.2011.06.062.

[24] B. Kalandyk, R. Zapała, Ł. Boroń, and M. Solecka, “Impact Strength of Austenitic and Ferritic-Austenitic Cr-Ni Stainless Cast Steel in -40 and +20°C Temperature,” *Archives of Metallurgy and Materials*, vol. 59, no. 3, pp. 1103–1106, Oct. 2014, doi: 10.2478/amm-2014-0190.

[25] S. Topolska and J. Labanowski, "Impact-toughness investigations of duplex stainless steels," *Mater. Tehnol.*, vol. 49, no. 4, pp. 481–486, Aug. 2015, doi: 10.17222/mit.2014.133.
[26] A. Busachi, J. Erkoyuncu, P. Colegrove, F. Martina, C. Watts, and R. Drake, "A review of Additive Manufacturing technology and Cost Estimation techniques for the defence sector," *CIRP Journal of Manufacturing Science and Technology*, vol. 19, pp. 117–128, Nov. 2017, doi: 10.1016/j.cirpj.2017.07.001.
[27] K. Derekar, J. Lawrence, G. Melton, A. Addison, X. Zhang, and L. Xu, "Influence of Interpass Temperature on Wire Arc Additive Manufacturing (WAAM) of Aluminium Alloy Components," *MATEC Web Conf.*, vol. 269, p. 05001, 2019, doi: 10.1051/matecconf/201926905001.
[28] B. Wu *et al.*, "A review of the wire arc additive manufacturing of metals: properties, defects and quality improvement," *Journal of Manufacturing Processes*, vol. 35, pp. 127–139, Oct. 2018, doi: 10.1016/j.jmapro.2018.08.001.
[29] B. Cong, Z. Qi, B. Qi, H. Sun, G. Zhao, and J. Ding, "A Comparative Study of Additively Manufactured Thin Wall and Block Structure with Al-6.3%Cu Alloy Using Cold Metal Transfer Process," *Applied Sciences*, vol. 7, no. 3, p. 275, Mar. 2017, doi: 10.3390/app7030275.
[30] E. M. Ryan, T. J. Sabin, J. F. Watts, and M. J. Whiting, "The influence of build parameters and wire batch on porosity of wire and arc additive manufactured aluminium alloy 2319," *Journal of Materials Processing Technology*, vol. 262, pp. 577–584, Dec. 2018, doi: 10.1016/j.jmatprotec.2018.07.030.
[31] Z. Jiang, H. Li, Z. Chen, Z. Huang, D. Zou, and L. Liang, "The Nitrogen Solubility in Molten Stainless Steel," *steel research international*, vol. 76, no. 10, pp. 740–745, Oct. 2005, doi: 10.1002/srin.200506090.